JPET Fast Forward. Published on September 26, 2016 as DOI: 10.1124/jpet.116.236562
This article has not been copyedited and formatted. The final version may differ from this version.

**JPET #236562**

# Akebia saponin D decreases hepatic steatosis through autophagy modulation

Li-li Gong, Guang-run Li, Wen Zhang, He Liu, Ya-li Lv, Fei-fei Han, Zi-Rui Wan, Ming-Biao Shi, Li-hong Liu*

*Beijing Chao-Yang Hospital, Capital Medical University, Beijing, China*

**JPET #236562**

**Running Title: Akebia saponin D decreases hepatic steatosis**

*Corresponding authors: Li-hong Liu, Li-li Gong. Beijing Chaoyang Hospital, Capital Medical University, 8 Gongren Tiyuchang Nanlu, Beijing 100020, China, Tel: 86-10-85231464; *E-mail address*: hongllh@126.com, gonglili@126.com.

The number of text pages: 29

The number of tables: 1

The number of figures: 8

The number of references: 26

The number of words in the Abstract: 190

The number of words in the Introduction: 484

The number of words in the Discussion: 865

**Abbreviations:**

NAFLD, Nonalcoholic fatty liver disease; HFD, high fat diet; DAW, Dipsacus asper Wall; ASD, Akebia saponin D; FBS, Fetal bovine serum; DMEM, Dulbecco's Modified Eagle Medium; OA, Oleic acid; CQ, Chloroquine; BSA, bovine serum albumin; AST, Aspartate transaminase; ALT, alanine transaminase; TG, Triglyceride; TC, Total cholesterol; FFA, Free Fatty Acids; HOMA-IR, Homeostasis model assessment of insulin resistance; SOD, superoxide dismutase; GSH-PX, glutathione peroxidase; MDA, malondialdehyde; SM, Silibinin meglumine.

**Recommended section assignment:** Drug Discovery and Translational Medicine

JPET Fast Forward. Published on September 26, 2016 as DOI: 10.1124/jpet.116.236562
This article has not been copyedited and formatted. The final version may differ from this version.



## Abstract

Nonalcoholic fatty liver disease (NAFLD) is considered to be a hepatic manifestation of metabolic syndrome, and its incidence is rapidly increasing. However, there is a lack of appropriate drugs for the therapy of NAFLD. In the present article, we aimed to elucidate the protective effects and mechanisms of Akebia saponin D (ASD) against NAFLD on ob/ob mice and BRL cells. ASD significantly decreased hepatic steatosis and heptocyte apoptosis in ob/ob mice. Furthermore, ASD significantly activated the autophagic flux assessed by decreased the expression of LC3-II, p62 accumulation of autophagosomes. In BRL cells, ASD prevented Oleic acid (OA) induced lipid droplets and increase the autophagic flux acting as increase the number of autolysosomes than autophagosomes in mTagRFP-mWasabi-LC3. ASD treatment also prevented OA induced LC3-II, p62, Beclin and phospho-mTOR expression. These effects were similar to the effects cotreatment with rapamycin. ASD treatment could not prevent the OA increased autophagy related protein expression after treated with Chloroquine (CQ) or siRNA-mediated knockdown of Atg7. These results suggest that Akebia saponin D alleviates hepatic steatosis targeted at the fusion of autophagosomes to lysosomes, autophagy modulation via ASD may offer a new strategy for treating NAFLD.

## Introduction

Nonalcoholic fatty liver disease (NAFLD) represents a spectrum of liver disease ranging from pure fatty liver through nonalcoholic steatohepatitis (NASH) to fibrosis and irreversible cirrhosis that occurs in patients who do not consume significant amounts of alcohol (Matteoni et al., 1999). NAFLD is strongly associated with components of the metabolic syndrome including obesity, hypertension, dyslipidemia and insulin resistance and, in fact, is now recognized to represent the hepatic manifestation of the metabolic syndrome (Smith and Adams, 2011). NAFLD occurs in developed and developing countries making NAFLD the most common liver condition in the world. Although a large number of studies have been conducted, the pathophysiology of NAFLD is complicatedand not completely elucidated.

NAFLD has been linked to lipid accumulation and lipid metabolism dysfunction. Recent studies have shown that autophagy is involved in lipid metabolism. Hepatic autophage degrades lipid droplets to provide FFA for ATP production when increase lipid availability. In contrast, hepatic autophagic turnover was inhibited if lipids were provided sustained by a long-lasting high fat diet (HFD). Singh et al. reported that lipid metabolism was regulated by autophagy through eliminating triglycerides and preventing development of steatosis (Singh et al., 2009). Decreased autophagic function may promote the initial development of hepatic steatosis (Czaja, 2010). It has been demonstrated that genetic leptin-deficient ob/ob mice, which show obesity andinsulin resistance developed NAFLD similar to that observed in human patients have been commonly used as an animal model of NAFLD. Many of the investigations pertaining to NAFLD are carried out in ob⁄ob mice. Studies in ob/ob mice have indicated that defective autophagy were observed (Yang et al., 2010). Autophagy

markers, as indicated by LC3-II accumulation and p62 degradation, were impaired in the liver of ob/ob mice. Consistently, autophagy-associated proteins such as Atg7, Beclin-1, and Atg5-Atg12 conjugation were downregulated. Therefore, activation of autophagy in hepatocytes could constitute a therapeutic approach against hepatic complications.

Akebia Saponin D (ASD, also named Asperosaponin VI) (Supplemental Figure 1) is a typical bioactive triterpenoid saponin isolated from the rhizome of Dipsacus asper Wall (DAW) which has long been used as an anti-osteoporosis drug (Yu et al., 2012). ASD has been demonstrated to have some therapeutic effects on some disease models such as cancer (Jeong et al., 2008), Alzheimer's disease (Jeong et al., 2008; Zhou et al., 2009; Yu et al., 2012), cardiovascular disease (Li et al., 2010a; Li et al., 2010b; Li et al., 2012) and bone fractures (Peng et al., 2010; Niu et al., 2011). Our previous studies have shown that ASD exerts the hepatoprotective effects on the acute liver injury induced by CCl4 in mice (Li Chao et al., 2012) and against rotenone-induced toxicity in liver BRL cells (Gong et al., 2014). These findings suggest ASD has the hepatoprotective effect. However, the beneficial effects of ASD on NAFLD have not been fully investigated. Therefore, in this study, the protective effect of ASD against NAFLD was investigated in leptin-deficient ob/ob mice and BRL cells.

## 2. Materials and methods

### *2.1 Drugs, reagents and plasmids*

ASD was extracted by Beijing Chao-Yang Hospital affiliated with Beijing Capital Medical University and its structure was confirmed by the basis of physical-chemical properties and spectral evidence (Yuan-yuan Lan et al., 2011). ASD standard (purity: 92.5%, Batch No. 11685-200802) was purchased from National institutes for Food

JPET Fast Forward. Published on September 26, 2016 as DOI: 10.1124/jpet.116.236562
This article has not been copyedited and formatted. The final version may differ from this version.



and Drug Control (Beijing, China). The purity of ASD was calculated based on external standard method. Briefly, the purity (%) = $\frac{\frac{C_{Standard}}{A_{Standard}} \times A_{Sample} \times V_{Sample}}{M_{Sample}} \times 100\%$, (C, concentration; A, peak area; M, sample weight). The purity of ASD was more than 98% tested by HPLC method (Supplemental Figure 2).

Silibinin meglumine (SM) was a generous gift from shanghai seebio biotech. Fetal bovine serum (FBS), Dulbecco's Modified Eagle Medium (DMEM) were obtained from Hyclone (Logan, Utah, USA). Oleic acid (OA), rapamycin, Chloroquine (CQ) and bovine serum albumin (BSA) were from Sigma-Aldrich (St. Louis, MO, USA). Immobilon PVDF membrane was purchased from Millipore (Billerica, MA, USA).

Aspartate transaminase (AST) and alanine transaminase (ALT) diagnostic biochemical assay kits were obtained from Biosino Biotechnology Company Ltd. (Beijing, China). Triglyceride (TG), Total cholesterol (TC), Free Fatty Acids (FFA), Fasting glucose, Fasting insulin, superoxide dismutase (SOD), glutathione peroxidase (GSH-PX) and malondialdehyde (MDA) diagnostic agents were obtained from Nanjing Jiancheng Bioengineering Institute (Nanjing, China).

Plasmids EGFP-LC3, mTagRFP-mWasabi-LC3 and mTagRFP-mWasabi-LC3□G were a generous gift from Prof. Jian Lin (Peking University). Microtubule associated protein light chain 3 (LC3) is a ubiquitin-like protein that binds to autophagosomes and subsequently EGFP tagged LC3 was used to track and follow the fate of autophagosomes in the cell. The plasmid mTagRFP-mWasabi-LC3 consists of a red fluorescent protein mTagRFP, a green fluorescent protein mWasabi and an amino terminal of the autophagy labeled protein LC3 which was used to monitoring autophagic flux. In green/red merged images, yellow puncta (i.e., RFP+, Wasabi+) indicate autophagosomes, while red puncta (i.e., RFP+, Wasabi-) indicate

JPET Fast Forward. Published on September 26, 2016 as DOI: 10.1124/jpet.116.236562
This article has not been copyedited and formatted. The final version may differ from this version.

autolysosomes. mTagRFP-mWasabi-LC3□G was constructed as the negative control.



### *2.2 Studies in ob/ob mice*

#### *2.2.1 Animals*

Six-week-old male C57BL/6 and leptin-deficient ob/ob mice were purchased from the Experimental Animal Center of the Fourth Military Medical University ( License: SCXK (JUN) 2007-007). The mice were housed individually under temperature (24 ± 5°C), humidity (55 ± 5%), and light (12 h light/dark cycle) controlled conditions. After acclimating for 1 week, nine C57BL/6 male mice were fed a standard purified rodent diet served as controls. The ob/ob mice were fed on high-fat diet (HFD) and randomly divided into five groups. The mice were administered vehicle (saline), ASD (30, 60 and 120 mg/kg/d) or Silibinin meglumine (SM, 20 mg/kg/d) through intraperitoneal injection for 4 weeks. All experiments were carried out in accordance with China Animal Welfare Legislation and were approved by Beijing Chao-Yang Hospital Committee on Ethics in the Care and Use of Laboratory Animals.

At the end of the experiment, the mice were anesthetized with urethane (1 g/kg, i.p.), the body weights, liver weights and fat pad weights were measured, blood samples were collected from inner canthus, and liver were removed immediately and washed in pre-chilled physiological saline. Levels of AST, ALT, fasting glucose and fasting insulin in blood, activity of SOD, MDA and GSH-PX and TG, TC, FFA levels in liver tissues were measured according to the manufacturer's instructionwith a SpectraMax M5 microplate reader (Molecular Devices, Sunnyvale, CA, USA). The homeostasis model assessment of insulin resistance (HOMA-IR) was estimated by dividing the product of fasting glucose (mmol/L) and insulin levels (mIU/L) by 22.5.

### *2.2.2 H&E stain*

The livers were washed immediately with saline and then fixed in 4% buffered paraformaldehyde solution. Paraffin-embedded liver biopsy sections (5 μm) were stained with hematoxylin and eosin (H&E) for histological analysis. These sections were examined under light microscope for histoarchitectural changes, and then photomicrographs were taken. The image-pro plus 6.0 software was used to evaluate the degree of hepatocellular ballooning and lobular inflammation (grade of activity).

### *2.2.3 Terminal deoxynucleotidyl transferase mediated dUTP nick end labeling (TUNEL) assay*

TUNEL assay was performed by using In Situ Cell Death Detection kit according to the manufacturer's instructions (POD, Roche Diagnostics Corporation, USA). For each liver, the total number of TUNEL-positive heptocyte nuclei was counted in ten sections. Individual nuclei were visualized at a magnification of 200, and the percentage of apoptotic nuclei (apoptotic nuclei/total nuclei) was calculated in 6 randomly chosen fields per slide and averaged for statistical analysis.

### *2.2.4 Electron Microscopy Ultrastructural examination*

Small pieces of liver were taken and rinsed in 0.1 M phosphate buffer solution (PBS, pH 7.2). Approximately, 1 mm3 liver pieces were trimmed and immediately fixed in ice-cold glutaraldehyde (3%) plus p-formaldehyde (4%) in 0.1 M phosphate buffer, and kept at 4 °C for 2 h. Samples were postfixed in 1% osmium tetroxide for 60 min at 25°C. After dehydration in a graded series of ethanol, liver pieces were embedded in spur resin. Thin sections (60 nm) were cut on an Ultramicrotome. The sectioned grids were stained with saturated solutions of uranyl acetate and lead citrate. The sections were examined by electron microscope (H-7650, Hitachi).

### *2.2.5 Immunohistochemistry*

The slides were stained with primary anti-LC3 antibody (Cell Signaling Technology, USA). Anti-rabbit HRP/DAB detection system was used to visualize the expression according to the protocol. Positive and negative controls were undertaken to identify any non-specific staining. For negative controls, the primary antibody was replaced by normal rabbit IgG (Vector Laboratories, Burlingame, CA, USA). All slides were viewed using an Olympus microscope.

### *2.2.6 Western blot analysis for autophagy*

Liver tissue lysates were subjected to SDS-PAGE and electrophoretically transferred to a polyvinylidene difluoride (PVDF) membrane. The membranes were then exposed to primary antibodies (LC3, p62, beclin, Cell Signaling Technology, USA) overnight at 4°C. After incubation with the IRDye 680LT secondary antibody (Licor, USA) for 1 h at room temperature, immunoreactive proteins were visualized by Odyssey Infrared Imaging System (LI-COR Biosciences, Lincoln, NE).

## *2.3 Studies in BRL cells*

### *2.3.1 Cell culture and treatment*

BRL cells, a cell line established from Buffalo rat liver, have been widely used for liver biological and chemical studies. BRL cells were purchased from the Cell Center of Shanghai Institutes for Biological Sciences (Shanghai, China). Cells were cultured in Dulbecco's Modified Eagle Medium (DMEM) supplemented with 10% (v/v) FBS at 37 °C with 5% $CO_2$. OA (20 mM) in 0.01 N NaOH was incubated at 70°C for 30 min, and then mixed with 10% BSA in PBS at a 1:9 molar ratio of OA to BSA. The OA-BSA conjugate was administered to the cultured cells. BSA was used as a vehicle control. BRL cells were pretreated with various concentrations of ASD (1, 10 and 100

μM) for 1 h, followed by incubation with 200 μM OA or vehicle control for 24 h. Rapamycin (25 ng/mL), chloroquine (CQ) (50 nM) were used as negative and positive control of autophagosome accumulation.

### *2.3.2 Lipid droplet staining*

BRL Cells were fixed in 4% paraformaldehyde in PBS for 30 minutes, washed thoroughly with PBS and incubated with specific neutral lipid probe Bodipy 493/503 (10 μg/mL; Invitrogen) at room temperature for 1 h in darkness. The cells were visualized under the fluorescence microscopy.

### *2.3.3 Cell culture and transfection*

BRL cells were cultured in Dulbecco's modified Eagle's medium (DMEM) (Hyclone) supplement with 10% FBS at 37°C in an atmosphere of 5% $CO_2$. About $1\times10^6$ cells were plated into confocal dish 24 h before transfection. EGFP-LC3 plasmids was usually used to detect autophagy. mTagRFP-mWasabi-LC3 reporter is sensitive and accurate in detecting the accumulation of autophagosomes and autolysosomes and used for monitoring autophagic flux. Meanwhile, mTagRFP-mWasabi-LC3□G was used as the negative control. Plasmids (EGFP-LC3, mTagRFP-mWasabi-LC3 and mTagRFP-mWasabi-LC3□G, 800 ng/well) transfections were performed with Lipofectamine 2000 (Invitrogen) according to the manufacturer's protocol (Zhou et al., 2012). The cells were ob served with confocal microscopy without fixation.

### *2.3.4 RNA interference*

BRL cells were transfected with siRNAs targeting Atg7 (GenePharma, Suzhou, China), or a control siRNA (GenePharma, Suzhou, China) using Lipofectamine 2000 (Invitrogen, Carlsbad, CA, USA) by following the manufacturer's instructions. Cells

were incubated for 16 h with a transfection mixture containing a final siRNA concentration of 100 pM, and then supplemented with fresh medium. RNA was extracted from cell culture lysates using TRIzol reagent (Invitrogen) according to standard protocol.

### *2.3.5 Real-time PCR analysis*

Real-time PCR analysis was used to quantify differences in gene expression. Target gene expression was normalized to that of an internal reference (GAPDH). Real-time PCR was performed with primers (Table II) and SYBR Premix Ex Taq (Takara, Japan) in Cobasz 480 real-time PCR machine (Roche). Target sequences were amplified by using the following thermal conditions: 2 min at 95°C, and 45 cycles of 10 s at 95°C and 30 s at 68°C. All reactions were performed in triplicate. The expression levels of the genes of interest were presented as the relative levels to the mRNA level of the control gene.

### *2.3.6 Western blot analysis*

Cells were harvested and lysed in protein lysis buffer (Applygen, Beijing, China). Proteins were separated in SDS-PAGE and transferred onto PVDF membranes. Membranes were incubated overnight at 4°C with the primary antibodies (Atg7, LC3 Cell Signaling Technology, USA). The membranes were washed and then incubated IRDye 680LT secondary antibody (Licor, USA) for 1 h at RT on an orbital shaker. After washing, bands were detected using Odyssey Infrared Imaging System (LI-COR Biosciences, Lincoln, NE).

### *2.4 Statistical analysis*

The results were expressed as means ± S.E.M in each group. To analyze the differences between groups, initial analyses were conducted with one-way ANOVA

tests followed by Dunnett's test. If the data did not fit the constraints of parametric test, data were analyzed with ChiSquare Test, Kruskal-Wallis ANOVA or the Mann-Whitney test. A value $P < 0.05$ was considered statistically significant.

## 3. Results

### *3.1 ASD treatment decreased plasma lipids and hepatic steatosis in ob/ob mice*

Body weights, liver weights and fat pad weights were calculated at the end of the experiments. We found that HFD ob/ob mice showed higher body weights, liver weights and fat pad weights compared with C57BL/6J mice. ASD treatment significantly inhibited the HFD-induced indices of adiposity and Liver/body weight in ob/ob mice.

The effects of ASD on glycemic control and insulin resistance are shown in Supplemental Table 1. Serum glucose levels were significantly lower in the ASD group than in the ob/ob mice group ($P < 0.05$). The serum insulin levels were significantly increased in the ob/ob group compared to the control group. ASD treatment significantly reduced the levels of these parameters ($p<0.05$). ASD significantly reduced the HOMA-IR value in comparison with the ob/ob mice group ($P < 0.01$).

The liver of ob/ob mice showed a marked accumulation of fat droplets, ballooning degeneration were also seen in the liver of ob/ob mice (Fig. 1B). ASD-treated obese mice displayed decreased hepatic steatosis (Fig. 1D-F). Livers of SM showed mild to moderate fat droplets (Fig. 1C). Likewise, hepatic triglyceride concentration decreased from 71.2 ± 3.5 mg/g in untreated obese mice to 38.6±1.8, 22.7±4.6, 14.3 ± 5.6 mg/g liver separately in ASD-treated animals ( $P < 0.001$ versus ob/ob mice) (Fig. 1G). In these mice, however, hepatic triglyceride content was significantly higher than

in wild-type mice (7.97 ± 5.2 mg/g wet liver; $P < 0.001$). The hepatic total cholesterol and FFA in ASD group were reduced compared with the ob/ob group ($P < 0.05$; Fig. H-I).

### *3.2 ASD treatment protected NAFLD-induced liver damage*

To test whether ASD could protect against NAFLD liver apoptosis, we performed TUNEL assays, ultrastructural examinaltion and hepatic AST, ALT, SOD, GSH-PX, MDA. The frequency of TUNEL-positive cells expressed as a percentage of the total nuclei was significantly increased in ob/ob mice (82.35 ± 2.14%), liver tissues demonstrated a marked appearance of dark brown apoptotic cells (Fig. 2Ab). In contrast, almost no apoptotic cells were observed in normal control C57BL/6J mice (Fig. 2Aa). Treatment with ASD (30, 60 and 120 mg/kg), the number of TUNEL positive cells was significantly decreased (40.28± 1.37%, 33.25 ± 1.20%, 22.39 ± 2.16%) (Fig. 2Cf).

The transmission electron micrograph studies of the hepatocyte nuclear of the experimental group were presented in Fig. 2B. In contrast to normal liver tissue (Fig. 2Ba), we found the hepatocyte shrinked and nucleolus broken (Fig. 2Bb). The electron micrograph of the nuclear of ASD (30, 60 and 120 mg/kg) treated mice showed less apoptosis in a dose-dependent manner. And the nuclear of liver tissue of ASD 120 mg/kg displayed near normal architecture.

Compared with the C57BL/6, the activities of serum hepatic injury marker enzymes aspartate transaminase (248.26±12.55) and alanine transaminase (346.18±20.35) were significant increase in ob/ob mice. Treatment with ASD (30, 60 and 120 mg/kg, respectively) almost restored all the alterations of aspartate transaminase (162.46±11.59, 145.69±12.70, 121.40±18.21), alanine transaminase (212.08±20.62,

176.24±19.97, 126.52±16.89) to near normal levels.

A significant rise in the content of malondialdehyde, as well as significant declines in the activity of superoxide dismutase and glutathione peroxidase was observed in the liver tissues of ob/ob mice. Administration of ASD (30, 60 and 120 mg/kg, respectively) markedly attenuated the alterations in antioxidant enzymes and maintained the mice at near normal status (Fig. 2Ca-e).

### *3.3 ASD treatment activated autophagy in liver tissue*

We performed electron microscopy to analyze autophagosome formation. The level of autophagosomes significant increased in the ASD (30, 60 and 120 mg/kg ) treated mice liver (Fig. 3A). Liver samples were also determine the immunohistological staining for LC3-II. Liver tissues taken from normal control C57BL/6J mice demonstrated little stain for LC3-II (Fig. 3Ba), ob/ob mice increased the degree of positive staining for LC3-II (Fig. 3Bb) whereas in ASD (30, 60 and 120 mg/kg) treated ob/ob mice LC3-II staining was significantly reduced (Fig. 3Bd-g). In addition, we also measured the levels of proteins that are specifically involved in autophagy. LC3-II, p62 and beclin levels were significantly increased in the ob/ob mice liver (Fig. 3C). On the contrary, ASD (30, 60 and 120 mg/kg) treatment decreased LC3-II, p62 and beclin expression.

### *3.4 ASD reduced hepatocyte lipid accumulation in BRL cells*

To further confirm the reduction hepatocyte lipid accumulation roles of ASD, we performed studies on BRL cells. As shown in Figure 4, BRL cells were fixed and stained with Bodipy 493/503, a fluorescent dye that specifically stains intracellular lipid droplets (LDs). OA treatment significantly increased the number of LDs in BRL cells. In contrast, LDs are barely detectable in BSA-treated control and very limited

lipid staining in the BRL cells was observed when treated with ASD (1, 10 and 100 μM).

### *3.5 ASD increased the autophagic flux*

We then determined the effects of ASD on OA-induced EGFP-LC3 puncta. We found that OA induced EGFP-LC3 puncta formation was significantly enhanced by ASD (1, 10 and 100 μM) (Fig. 5A). In addition to monitoring autophagosomes, assays for monitoring autophagic flux are also developed and mTagRFP-mWasabi-LC3 plasmid was used. In green/red merged images, yellow puncta indicate autophagosomes,

while red puncta indicate autolysosomes. In BRL cells treated with ASD (1, 10 and 100 μM), ASD increased more autolysosomes than autophagosomes, indicating autophagic flux in cells (Fig. 5B).

### *3.6 Molecular evidence for autophagy induction by ASD*

We next measured the expression of autophagy-related proteins LC3-II, p62, Beclin and mTOR in BRL cells.

OA treatment of BRL cells resulted in an increase in LC3-II (Fig. 6Aa). We also found that accumulation of p62 was paralleled to an increase in the LC3-II, reflecting a loss of the autophagic flux (Fig. 6Aa). In addition, the levels of Beclin expression and the phosphorylation levels of mTOR were also increased following the OA treatment. ASD (100 μM) treatment prevented the OA induced LC3-II, p62, Beclin and phospho-mTOR expression. Under the same experimental conditions, rapamycin decreased p62 and LC3-II/LC3-I ratio in OA-treated cells as compared with cells treated with OA alone, indicating a recovery of the autophagic flux (Fig. 6Ab). ASD (100 μM) treatment exhibited almost the same effect of rapamycin (Fig. 6Ab). ASD (100 μM) treatment could not attenuate the autophagic flux blocked by CQ (Fig.

6Ac).



BRL cells were infected with siRNAs targeting autophagy gene Atg7 or with a control siRNA. Levels of Atg7 were markedly decreased on immunoblots in siAtg7 cells in parallel with reduced levels of LC3-II, compatible with a decrease of autophagic function (Fig. 6B). The effect of ASD on cell lipid droplets was measured in the presence of siAtg7. Knockdown of Atg7 abolished the protective effect of ASD. LDs significantly increased in the presence of siAtg7 also when treated with OA and ASD (Fig. 6Bc). LC3-II levels decreased markedly in siAtg7 cells but not siControl cells and cells treated with OA and ASD. The levels of LC3-II decreased because

interference of autophagy gene Atg7 inhibited the formation of autophagosomes. Chloroquine (CQ) increased the levels of LC3-II as it targeted at inhibited the fusion of autophagosomes to lysosomes. ASD treatment could not prevent the OA induced p62, Beclin and phospho-mTOR expression.

## 4. Discussion

The pathogenesis of NAFLD has not yet been fully understood, but studies on ob/ob mice and oleic acid induced BRL cells lipid accumulation provide a good insight into this pathology. In the present study, we found that Akebia saponin D exerted a strong hepatoprotective effect against NAFLD. Autophagy may contribute to its hepatoprotective effect. During the past recent years, it has been reported that autophgy plays an important role in hepatic steatosis (Amir and Czaja, 2011; Gracia-Sancho et al., 2014; Kwanten et al., 2014; Lavallard and Gual, 2014). Enhancing autophagy by overexpressing an autophagy gene Atg7, could improve hepatic steatosis in ob/ob mice and in high fat diet-fed mice (Yang et al., 2010). The similar

results were also observed in high fat diet-induced non-alcoholic fatty liver condition when treated with mTOR inhibitor rapamycin (Lin et al., 2013).



In the present study, we found that Akebia saponin D treatment could signifiantly reduce liver weight, hepatic steatosis, hepatic triglyceride levels, total cholesterol and FFA levels. ASD treatment showed reduced hepatocyte nucleolus broken and shrinked. We also demonstrated that treatment with ASD attenuated the degree of apoptosis, increase the level of AST, ALD and the activity of SOD, GSH-PX and decrease MDA. These results suggest that ASD exerted a protective effect against NAFLD. ASD treated mice showed decreased body weight, Fat pad weight and HOMA-IR values. NAFLD is the hepatic manifestation of metabolic syndrome. As such, it is possible that ASD may have positive impacts on systemic components of the disease.

High-fat diet ob/ob mice showed impairment in the hepatic autophagic function. The protein amount of p62 was accumulated within the liver of ob/ob mice in parallel with an increase in the LC3-II indicated that function of autophagy was diminished in ob/ob mice liver. ASD treatment decreased LC3-II and p62 expression. The level of autophagosomes also significantly increased in the ASD treated mice liver. It has been shown that an accumulation of p62 reflects a decrease in the autophagic flux and contrarily activation of the autophagic flux leads to a decline in p62 expression (Bjorkoy et al., 2005; Klionsky et al., 2012). The accumulation of LC3-II and autophagosomes may be interpreted as induction of autophagy or a consequence of a blockade of the autophagic flux (Gonzalez-Rodriguez et al., 2014). Therefore, it is conceivable that the decreased of LC3-II and p62 expression which was observed when treated with ASD could be reflecting an activation of autophagic flux.

To further confirm the reduction hepatic steatosis and activation of autophagic flux roles of ASD, we performed studies on BRL cells. Oleic acid induced lipotoxicity has



a critical role in the pathogenesis of NAFLD. With the administration of ASD a decrease of lipid droplets was observed. EGFP-LC3 fluorescence studies are convenient methods to detect autophagy. ASD significantly enhanced EGFP-LC3 puncta indicating that ASD increased cell autophagy. mTagRFP-mWasabi-LC3 reporter is then used to detect the accumulation of autophagosomes and autolysosomes and used for monitoring autophagic flux. Autophagic flux is increased when both yellow and red puncta are increased in cells while autophagic flux is blocked when only yellow puncta are increased without an accompanying increase of red puncta in cells [17]. In the present study, we found that treated with ASD, more autolysosomes was increased than autophagosomes, indicating autophagic flux was increased.

OA treatment of BRL cells resulted in an accumulation of p62 paralleled with an increase in the LC3-II, reflecting a loss of the autophagic flux. ASD prevented OA induced LC3-II, p62, Beclin and phospho-mTOR expression. The activation of the autophagy machinery of ASD was demonstrated on several levels, including examining LC3-II, p62, Beclin and phospho-mTOR expression in the absence or presence of rapamycin or CQ. In the present study, we found that ASD can attenuate the autophagic flux blocked by OA reflected by reduced phosphorylation of mTOR, decreased p62, LC3-II and similar to the effect of rapamycin. Regarding autophagy-induced clearance of hepatic lipid droplets, ASD was no longer able to alleviate lipid accumulation in the presence of siRNA-mediated knockdown of Atg7. Moreover, depletion of Atg7 or treated with CQ abolished the protective effect of ASD act as

JPET Fast Forward. Published on September 26, 2016 as DOI: 10.1124/jpet.116.236562
This article has not been copyedited and formatted. The final version may differ from this version.

could not decrease LC-II and p62 levels. These data, point to a critical requirement of autophagic flux in the decreased of lipid droplets actions of ASD.



How do ASD increase autophagic flux? Several mechanisms may lead to increased autophagic flux, which include: (1) promotion of the upstream induction of autophagy and autophagosome biogenesis; or (2) increasing of autophagosomal-lysosomal fusion (Manley et al., 2014). We found that ASD-treatment decreased LC3-II and p62 levels; therefore, it is less likely that ASD promote upstream autophagosome biogenesis. Therefore it is likely that ASD might improve autophagic flux by increasing autophagosomal-lysosomal fusion. Indeed, we found that ASD not only increased EGFP-LC3 puncta but also increased the yellow and red puncta in tandem mTagRFP-mWasabi-LC3 assay which could eventually lead to increased autophagosomallysosomal fusion.

In conclusion, our results indicate that Akebia saponin D mediated alleviation of increased hepatic steatosis targeted at the fusion of autophagosomes to lysosomes. Activation of autophagy in hepatocytes could constitute a therapeutic approach against hepatic steatosis. These results strongly suggest that autophagy modulation via ASD may offer a new strategy for treating NAFLD.

## Conflict of interest statement

We declare that we have no conflict of interest.

## Acknowledgements

We would like to thank professor Jian Lin for providing plasmids of EGFP-LC3, mTagRFP-mWasabi-LC3 and mTagRFP-mWasabi-LC3□G.

## Authorship Contributions

Participated in research design: Gong LL and Liu LH.

Conducted experiments: Gong LL, Li GR and Zhang W.



Contributed reagents or analytic tools: Liu H and Shi MB.

Performed data analysis: Lv YL, Han FF, Wan ZR.

Wrote or contributed to the writing of the manuscript: Gong LL and Li GR.

## References

Amir M and Czaja MJ (2011) Autophagy in nonalcoholic steatohepatitis. *Expert review of gastroenterology & hepatology* **5**:159-166.

Bjorkoy G, Lamark T, Brech A, Outzen H, Perander M, Overvatn A, Stenmark H and Johansen T (2005) p62/SQSTM1 forms protein aggregates degraded by autophagy and has a protective effect on huntingtin-induced cell death. *The Journal of cell biology* **171**:603-614.

Czaja MJ (2010) Autophagy in health and disease. 2. Regulation of lipid metabolism and storage by autophagy: pathophysiological implications. *American journal of physiology* **298**:C973-978.

Gong LL, Wang ZH, Li GR and Liu LH (2014) Protective effects of akebia saponin d against rotenone-induced hepatic mitochondria dysfunction. *Journal of pharmacological sciences* **126**:243-252.

Gonzalez-Rodriguez A, Mayoral R, Agra N, Valdecantos MP, Pardo V, Miquilena-Colina ME, Vargas-Castrillon J, Lo Iacono O, Corazzari M, Fimia GM, Piacentini M, Muntane J, Bosca L, Garcia-Monzon C, Martin-Sanz P and Valverde AM (2014) Impaired autophagic flux is associated with increased endoplasmic reticulum stress during the development of NAFLD. *Cell death & disease* **5**:e1179.

Gracia-Sancho J, Guixe-Muntet S, Hide D and Bosch J (2014) Modulation of autophagy for the treatment of liver diseases. *Expert opinion on investigational drugs* **23**:965-977.

Jeong SI, Zhou B, Bae JB, Kim NS, Kim SG, Kwon J, Kim DK, Shin TY, Jeon H, Lim JP, Kim H, Kim HK and Oh CH (2008) Apoptosis-inducing effect of

akebia saponin D from the roots of Dipsacus asper Wall in U937 cells. *Archives of pharmacal research* **31**:1399-1404.

Klionsky DJ, Abdalla FC, Abeliovich H, Abraham RT, Acevedo-Arozena A, Adeli K, Agholme L, Agnello M, Agostinis P, Aguirre-Ghiso JA, Ahn HJ, Ait-Mohamed O, Ait-Si-Ali S, Akematsu T, Akira S, Al-Younes HM, Al-Zeer MA, Albert ML, Albin RL, Alegre-Abarrategui J, Aleo MF, Alirezaei M, Almasan A, Almonte-Becerril M, Amano A, Amaravadi R, Amarnath S, Amer AO, Andrieu-Abadie N, Anantharam V, Ann DK, Anoopkumar-Dukie S, Aoki H, Apostolova N, Arancia G, Aris JP, Asanuma K, Asare NY, Ashida H, Askanas V, Askew DS, Auberger P, Baba M, Backues SK, Baehrecke EH, Bahr BA, Bai XY, Bailly Y, Baiocchi R, Baldini G, Balduini W, Ballabio A, Bamber BA, Bampton ET, Banhegyi G, Bartholomew CR, Bassham DC, Bast RC, Jr., Batoko H, Bay BH, Beau I, Bechet DM, Begley TJ, Behl C, Behrends C, Bekri S, Bellaire B, Bendall LJ, Benetti L, Berliocchi L, Bernardi H, Bernassola F, Besteiro S, Bhatia-Kissova I, Bi X, Biard-Piechaczyk M, Blum JS, Boise LH, Bonaldo P, Boone DL, Bornhauser BC, Bortoluci KR, Bossis I, Bost F, Bourquin JP, Boya P, Boyer-Guittaut M, Bozhkov PV, Brady NR, Brancolini C, Brech A, Brenman JE, Brennand A, Bresnick EH, Brest P, Bridges D, Bristol ML, Brookes PS, Brown EJ, Brumell JH, et al. (2012) Guidelines for the use and interpretation of assays for monitoring autophagy. *Autophagy* **8**:445-544.

Kwanten WJ, Martinet W, Michielsen PP and Francque SM (2014) Role of autophagy in the pathophysiology of nonalcoholic fatty liver disease: a controversial issue. *World J Gastroenterol* **20**:7325-7338.

Lavallard VJ and Gual P (2014) Autophagy and non-alcoholic fatty liver disease. *BioMed research international* **2014**:120179.

Li C, Gao Y, Tian J, Xing Y, Zhu H and Shen J (2012) Long-term oral Asperosaponin VI attenuates cardiac dysfunction, myocardial fibrosis in a rat model of chronic myocardial infarction. *Food Chem Toxicol* **50**:1432-1438.

Li C, Liu Z, Tian J, Li G, Jiang W, Zhang G, Chen F, Lin P and Ye Z (2010a) Protective roles of Asperosaponin VI, a triterpene saponin isolated from Dipsacus asper Wall on acute myocardial infarction in rats. *European journal of pharmacology* **627**:235-241.

Li C, Tian J, Li G, Jiang W, Xing Y, Hou J, Zhu H, Xu H, Zhang G, Liu Z and Ye Z (2010b) Asperosaponin VI protects cardiac myocytes from hypoxia-induced apoptosis via activation of the PI3K/Akt and CREB pathways. *European journal of pharmacology* **649**:100-107.

Li Chao, Zhang Xiao-Fei, Lv Ya-Li, Lan Yuan-Yuan, Lei Ning and Li-Hong L (2012) Hepatoprotective effect of akebia saponin D on the acute liver injury induced by CCl4 in mice. *West China Journal of Pharmaceutical Sciences* **27**:257-259.

Lin CW, Zhang H, Li M, Xiong X, Chen X, Chen X, Dong XC and Yin XM (2013) Pharmacological promotion of autophagy alleviates steatosis and injury in alcoholic and non-alcoholic fatty liver conditions in mice. *Journal of hepatology* **58**:993-999.

Manley S, Ni HM, Kong B, Apte U, Guo G and Ding WX (2014) Suppression of autophagic flux by bile acids in hepatocytes. *Toxicological sciences : an official journal of the Society of Toxicology* **137**:478-490.

Matteoni CA, Younossi ZM, Gramlich T, Boparai N, Liu YC and McCullough AJ (1999) Nonalcoholic fatty liver disease: a spectrum of clinical and pathological severity. *Gastroenterology* **116**:1413-1419.

Niu Y, Li Y, Huang H, Kong X, Zhang R, Liu L, Sun Y, Wang T and Mei Q (2011) Asperosaponin VI, a saponin component from Dipsacus asper wall, induces osteoblast differentiation through bone morphogenetic protein-2/p38 and extracellular signal-regulated kinase 1/2 pathway. *Phytother Res* **25**:1700-1706.

Peng LH, Ko CH, Siu SW, Koon CM, Yue GL, Cheng WH, Lau TW, Han QB, Ng KM, Fung KP, Lau CB and Leung PC (2010) In vitro & in vivo assessment of a herbal formula used topically for bone fracture treatment. *Journal of ethnopharmacology* **131**:282-289.

Singh R, Kaushik S, Wang Y, Xiang Y, Novak I, Komatsu M, Tanaka K, Cuervo AM and Czaja MJ (2009) Autophagy regulates lipid metabolism. *Nature* **458**:1131-1135.

Smith BW and Adams LA (2011) Non-alcoholic fatty liver disease. *Critical reviews in clinical laboratory sciences* **48**:97-113.

Yang L, Li P, Fu S, Calay ES and Hotamisligil GS (2010) Defective hepatic autophagy in obesity promotes ER stress and causes insulin resistance. *Cell metabolism* **11**:467-478.

Yu X, Wang LN, Ma L, You R, Cui R, Ji D, Wu Y, Zhang CF, Yang ZL and Ji H (2012) Akebia saponin D attenuates ibotenic acid-induced cognitive deficits and pro-apoptotic response in rats: involvement of MAPK signal pathway. *Pharmacology, biochemistry, and behavior* **101**:479-486.

Yuan-yuan Lan, Ning Lei, Xiao-Fei Zhang, Run-tao Yang, Chao Li and L-H. L (2011) Hypolipidemic function with liver protection of extracts from Dipsacus asper on nonalcoholic fatty liver diseas e in mice and its activie fractions. *Chinese Traditional and Herbal Drugs* **42**:2497-2501.

Zhou C, Zhong W, Zhou J, Sheng F, Fang Z, Wei Y, Chen Y, Deng X, Xia B and Lin J (2012) Monitoring autophagic flux by an improved tandem fluorescent-tagged LC3 (mTagRFP-mWasabi-LC3) reveals that high-dose rapamycin impairs autophagic flux in cancer cells. *Autophagy* **8**:1215-1226.

Zhou YQ, Yang ZL, Xu L, Li P and Hu YZ (2009) Akebia saponin D, a saponin component from Dipsacus asper Wall, protects PC 12 cells against amyloid-beta induced cytotoxicity. *Cell biology international* **33**:1102-1110.

## Footnotes

This study was supported by the National Natural Science Foundation of China (No.81302822). Beijing Municipal Administration of Hospitals' Youth Programme (No. QML20150302). The capital of Chinese medicine research subject (No. 15ZY02).

## Figure legend

Fig.1. Effects of ASD on liver morphology in ob/ob mice. (A) C57BL/6 mice showed normal hepatocytes with distinctive membrane, abundant cytoplasm and regular oval nuclei. (B) ob/ob mice treated with saline i.p. for 4 wk showed a marked accumulation of fat droplets; (C) ob/ob mice treated with Silibinin meglumine (SM, 20 mg/kg/d) for 4 wk showed mild to moderate the fat droplets; (D–F) ob/ob mice treated with ASD (30, 60 and 120 mg/kg/d) i.p. for the same period of time. ASD-treated obese mice displayed decreased hepatic steatosis. H&E stain 100× (Scale bar: 400 μm.) and 400× (Scale bar: 200 μm.). (G-I) Liver triglyceride, total cholesterol, free fatty acids concentration, ASD-treated significantly decreased hepatic TG, TC, FFA level. Results are presented as means ± S.E.M., n = 6, Compared with normal control: ##P < 0.01; compared with ob/ob mice: **P < 0.01.

Fig. 2. Effect of ASD on heptocyte apoptosis in ob/ob mice. (Aa and Ba) Normal group no apoptotic cells. (Ab and Bb) ob/ob mice treated with saline i.p. for 4 wk showed significantly more TUNEL positive apoptotic cells, TEM showed hepatocyte shrinked and nucleolus broken (b) and the increase in apoptotic cells is significantly attenuated by ASD (30, 60 and 120 mg/kg/d, respectively) treatment (d-f). (Ac and Bc) SM 20 mg/kg/d also decreased the apoptotic cells. Effect of ASD on serum marker enzymes aspartate transaminase (AST) and alanine transaminase (ALT) in ob/ob mice (Ca-b). Effect of ASD on liver levels of superoxide dismutase (SOD), malondialdehyde (MDA), and glutathione peroxidase (GSH-PX) in ob/ob mice (Cc-e). Effects of ASD on the number of TUNEL positive cells (Cf). TUNEL scale bar: 100 μm, TEM scale bar: 50 μm. Results are presented as means ± S.E.M., n = 6,

Compared with normal control: ##P < 0.01; compared with ob/ob mice: **P < 0.01.

Fig. 3. Effects of ASD on autophagy in ob/ob mice liver. (A) Electron microscopy shows the ultrastructure of mice liver. Arrows indicate autophagosomes. Scale bar: 20 μm. (B) Immunohistochemistry for LC3-II. Scale bar: 100 μm. (C) Western blot analysis of the levels of LC3-II, p62 and beclin. All values are means ± S.E.M., n = 6, Compared with normal control: ##P < 0.01; compared with ob/ob mice: * P < 0.05, **P < 0.01.

Fig.4. ASD reduces oleic acid-induced lipid accumulation in BRL cells. Treatment with OA (200 μM) significantly increased intracellular lipid accumulation (B). In contrast, pretreatment with ASD (1, 10 and 100 μM) for 1 h before OA exposure significantly reduced OA-induced lipid accumulation, as assessed by visualization of bodipy 493/503 staining (C-E). Scale bar: 100 μm.

Fig.5. ASD increased the autophagic flux. Representative fluorescent images of BRL cells transiently transfected with EGFP-LC3. Quantitation of autophagic cells based on % EGFP-LC3 positive cells with EGFP-LC3 dots. (A), mTagRFP-mWasabi-LC3(B), mTagRFPmWasabi-LC3△G (C). Comparison of both green and red fluorescent signals of mTagRFP-mWasabi-LC3 in different conditions. Cells with autolysosomes and/or autolysosomes were samples from a pool of at least 10 images. Scale bar: 50 μm.

Fig.6. Effect of ASD on autophagy-related proteins in OA induced lipid accumulation

BRL cells. (Aa) Total protein was isolated from BRL cells when treated with ASD (1,



10, 100 μM) and immunoblotted with antibodies for phospho-mTOR, p62, beclin, LC3, and β-actin. (Ab) Immunoblots of proteins isolated from Rapamycin (25 ng/mL) and/or ASD (100 μM) treated BRL cells and probed with the antibodies shown. (Ac) Immunoblots were conducted in BRL cells treated with chloroquine (CQ) (50 nM) and/or ASD (100 μM).

Effect of ASD on lipid accumulation when inhibited the autophagy. (Ba) Quantification of Atg7 after transfection with control or Atg7 siRNA. (Bb) Western blots of lysates from BRL cells knocked down with Atg7 siRNA. (Bc) Bodipy 493/503 staining of OA and ASD treated BRL cells after transfection with control or Atg7 siRNA. Scale bar: 200 μm. (Bd) Immunoblots of proteins isolated from siControl and siAtg7 cells and probed with the antibodies shown. All values are means ± S.E.M. from three or more independent studies. *$P < 0.05$; **$P < 0.01$.

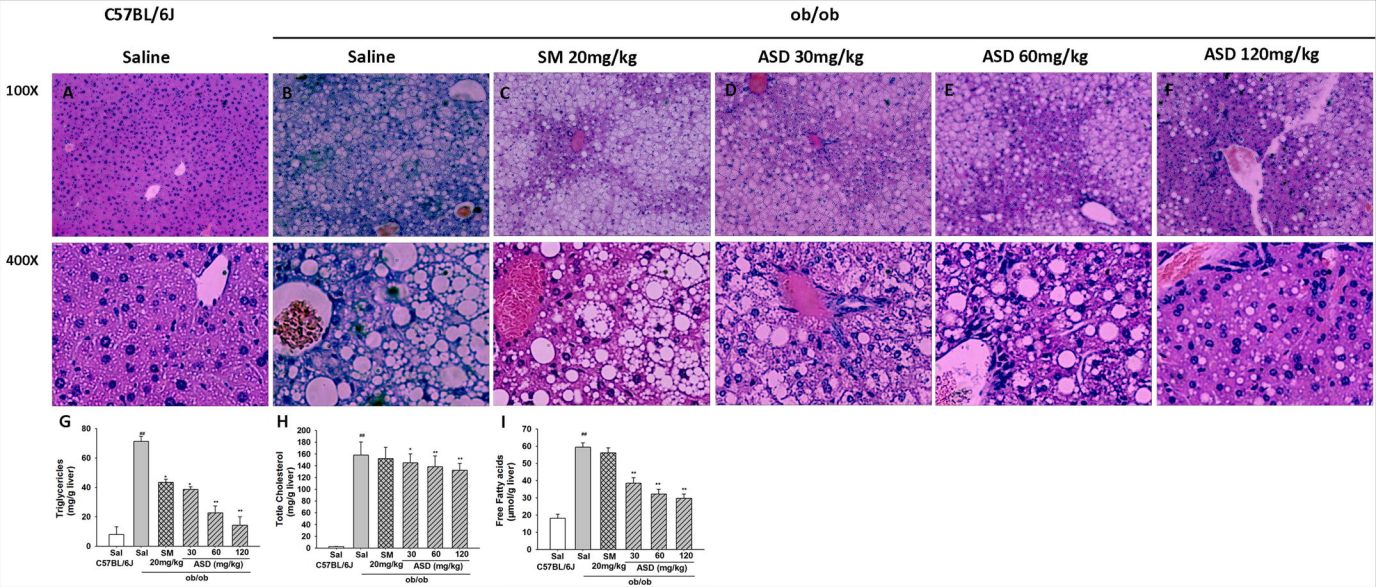
C57BL/6J
ob/ob
Saline
Saline
SM 20mg/kg
ASD 30mg/kg
ASD 60mg/kg
ASD 120mg/kg
100X
400X
A
B
C
D
E
F
G
Triglycericles (mg/g liver)
H
Totle Cholesterol (mg/g liver)
I
Free Fatty acids (μmol/g liver)
Sal
SM
30
60
120
20mg/kg
ASD (mg/kg)
C57BL/6J
ob/ob

Figure 2

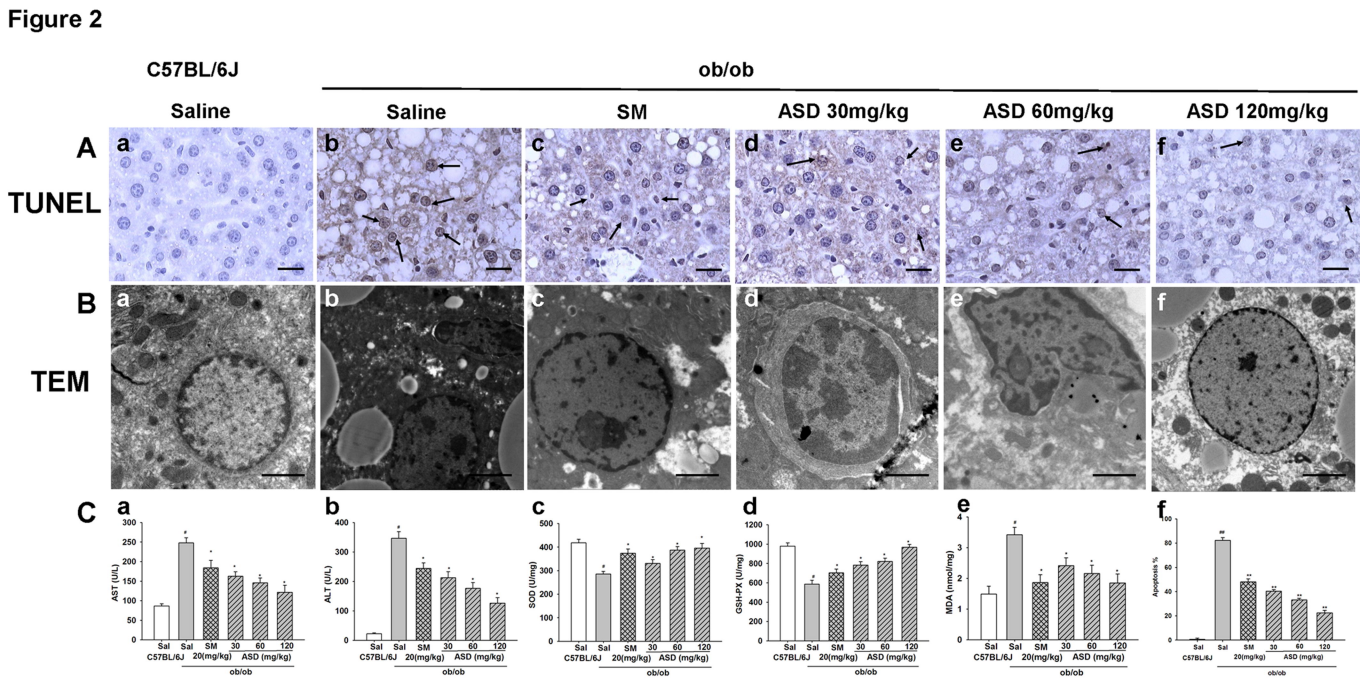
C57BL/6J
ob/ob
Saline
Saline
SM
ASD 30mg/kg
ASD 60mg/kg
ASD 120mg/kg
A
TUNEL
a
b
c
d
e
f
B
TEM
a
b
c
d
e
f
C
a
AST (U/L)
b
ALT (U/L)
c
SOD (U/mg)
d
GSH-PX (U/mg)
e
MDA (nmol/mg)
f
Apoptosis %
Sal
Sal
SM
30
60
120
C57BL/6J
20(mg/kg)
ASD (mg/kg)
ob/ob

Figure 3

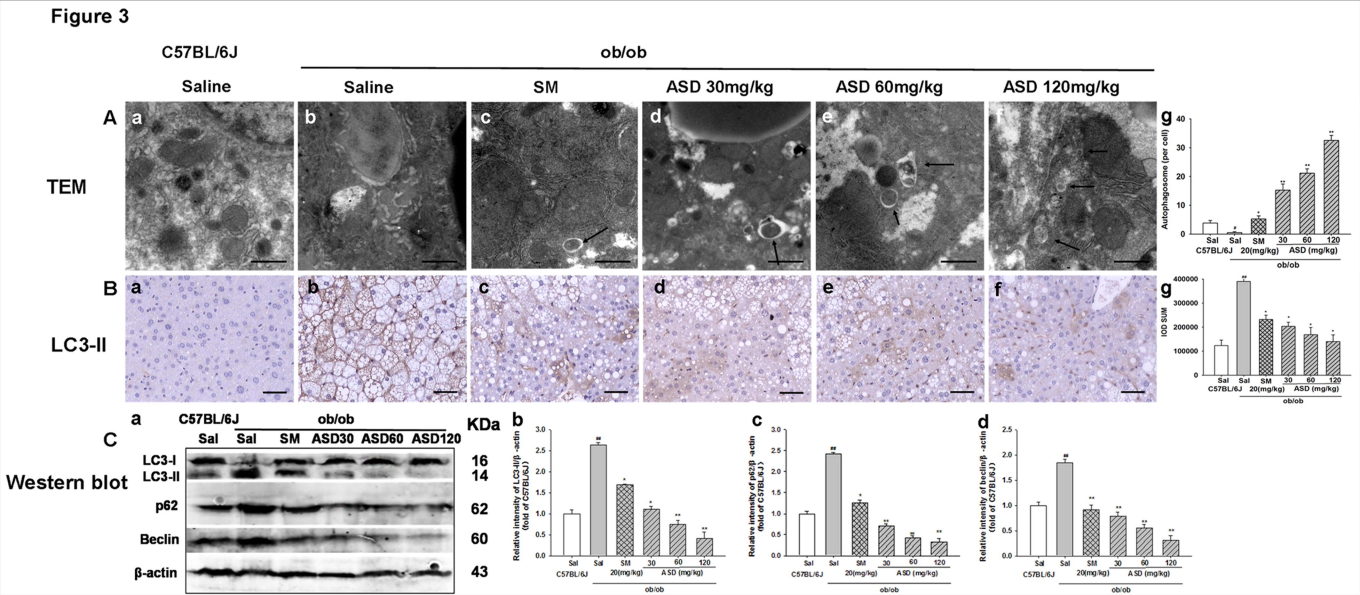
C57BL/6J
ob/ob
Saline
Saline
SM
ASD 30mg/kg
ASD 60mg/kg
ASD 120mg/kg
A
TEM
a
b
c
d
e
f
g
Autophagosome (per cell)
Sal
Sal
SM
30
60
120
C57BL/6J
20(mg/kg)
ASD (mg/kg)
ob/ob
B
LC3-II
IOD SUM
C
Western blot
a
C57BL/6J
ob/ob
KDa
Sal
Sal
SM
ASD30
ASD60
ASD120
LC3-I
LC3-II
p62
Beclin
β-actin
16
14
62
60
43
b
c
d
Relative intensity of LC3-II/β -actin (fold of C57BL/6J)
Relative intensity of p62/β -actin (fold of C57BL/6J)
Relative intensity of beclin/β -actin (fold of C57BL/6J)

Figure 4

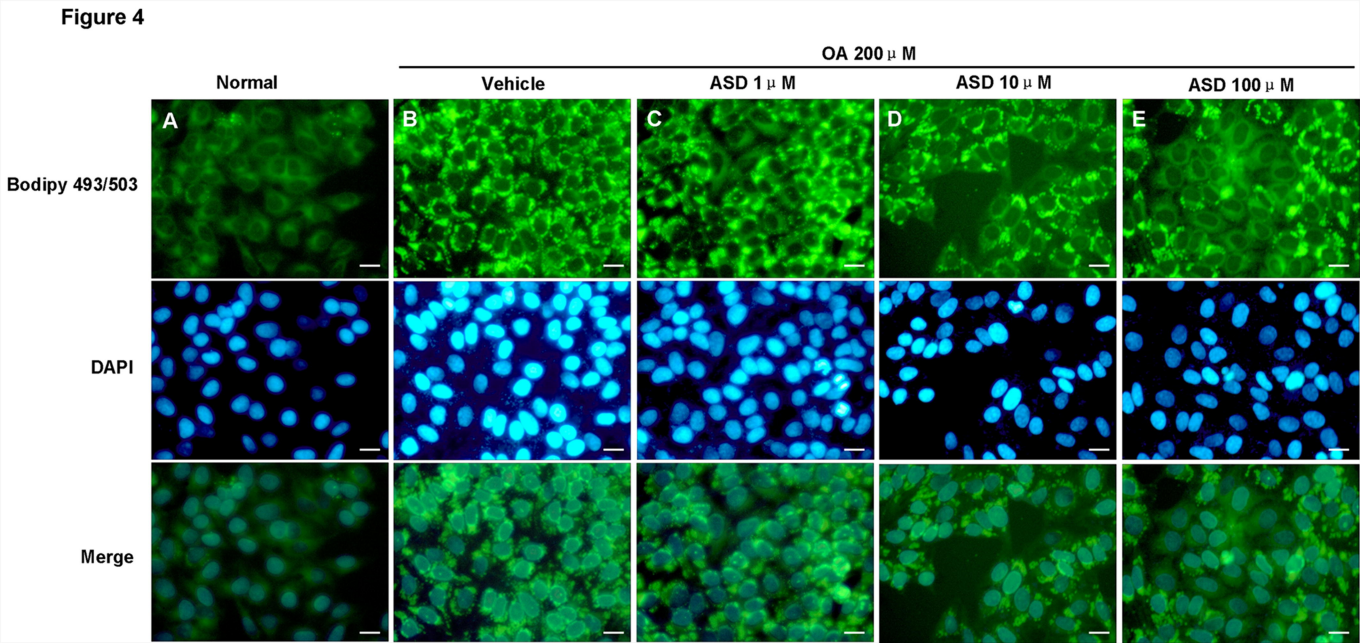
OA 200 μ M
Normal
Vehicle
ASD 1 μ M
ASD 10 μ M
ASD 100 μ M
A
B
C
D
E
Bodipy 493/503
DAPI
Merge

Figure 5

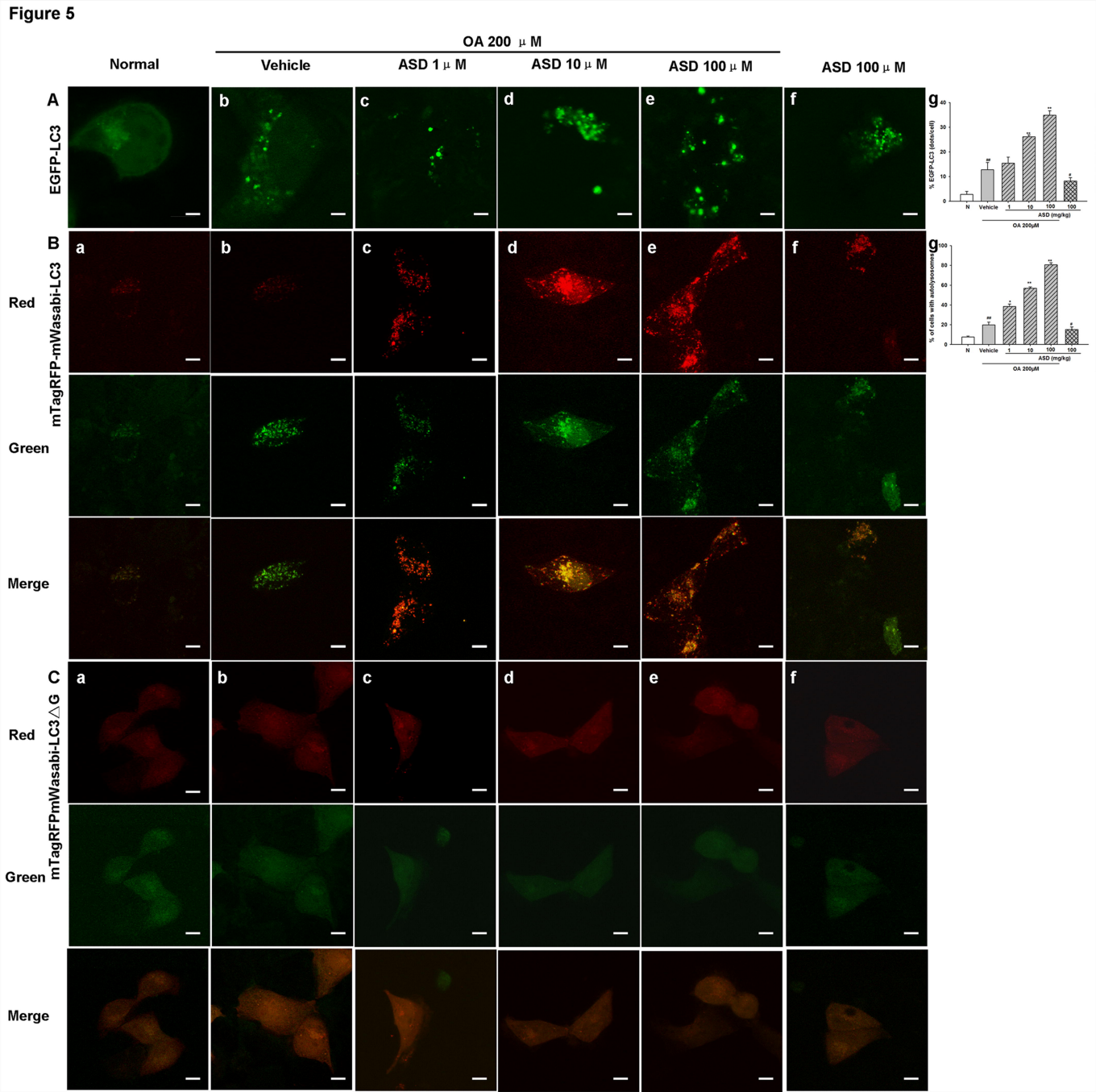
OA 200 μM
Normal
Vehicle
ASD 1 μM
ASD 10 μM
ASD 100 μM
ASD 100 μM
A
EGFP-LC3
B
Red
mTagRFP-mWasabi-LC3
Green
Merge
C
Red
mTagRFPmWasabi-LC3△G
Green
Merge
g
% EGFP-LC3 (dots/cell)
N
Vehicle
1
10
100
100
ASD (mg/kg)
OA 200μM
g
% of cells with autolysosomes
N
Vehicle
1
10
100
100
ASD (mg/kg)
OA 200μM

Figure 6

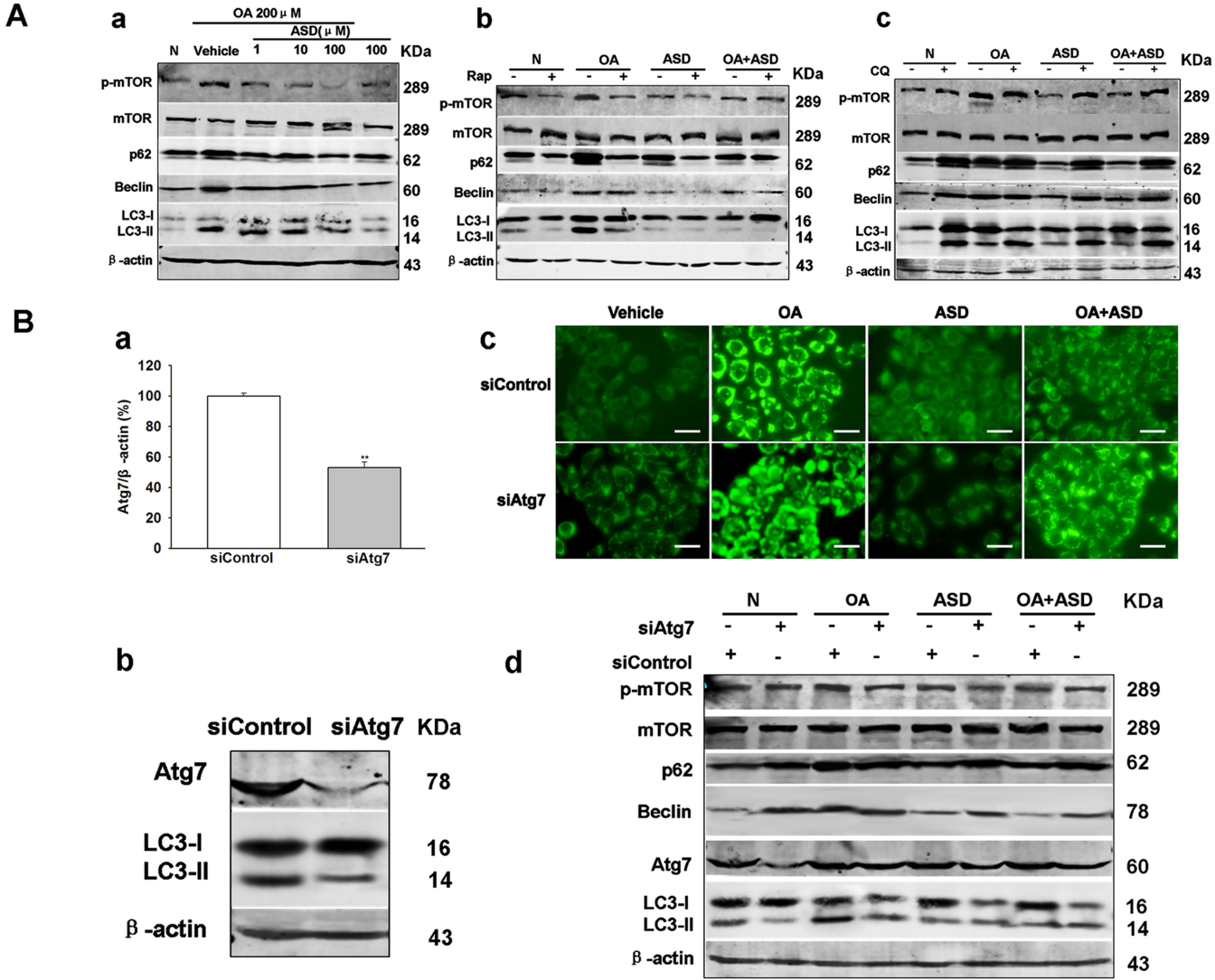
A
a
OA 200 μ M
ASD( μ M)
N
Vehicle
1
10
100
100
KDa
p-mTOR
mTOR
p62
Beclin
LC3-I
LC3-II
β -actin
289
289
62
60
16
14
43
b
Rap
N
OA
ASD
OA+ASD
KDa
c
CQ
B
a
Atg7/β -actin (%)
120
100
80
60
40
20
0
**
siControl
siAtg7
b
siControl
siAtg7
KDa
Atg7
78
c
Vehicle
OA
ASD
OA+ASD
siControl
siAtg7
d
siAtg7
siControl
Beclin
60
78